Micrometer Scale Y–Ba–Cu–O SQUID Arrays Fabricated With a Focused Helium Ion Beam

Ethan Y. Cho, Member, IEEE, Jay C. LeFebvre, R. C. Dynes, and Shane A. Cybart, Senior Member, IEEE

Abstract—We present the fabrication and testing of microarrays of superconducting quantum interference devices (SQUIDs) fabricated from the high-transition temperature superconductor $YBa_2Cu_3O_{7-\delta}$ (YBCO). The arrays consisted of 84 SQUIDs, each with loop area 25 μ m², connected electrically in series with a meander line structure. The entire array was contained in an area of just 100 μ m \times 100 μ m. The Josephson junctions in the arrays were directly written into YBCO thin films with ion irradiation from a focused helium ion beam. We found that the electrical properties can be controlled by changing the diameter of the ion beam through selection of either a 20 or 5 μ m beam aperture. In particular, larger aperture or beam size results in a weaker link junction with higher operating temperature and smaller critical voltage. The voltages across the dc-biased arrays were measured as a function of magnetic field. The data exhibited maximum voltage modulations of 300 μV at 65 K and 1 mV at 52 K for the 20 and 5 μ m beam aperture, respectively. The magnetic field periodicity for both arrays was approximately 30 μ T per flux quantum.

Index Terms—Focused helium ion beam (He-FIB), superconducting quantum interference devices (SQUIDs), SQUID array, YBa $_2$ Cu $_3$ O $_{7-\delta}$ (YBCO).

I. INTRODUCTION

HERE has been a great deal of interest in arrays of superconducting quantum interference devices (SQUIDs) for magnetic sensors exhibiting, low noise, high sensitivity, and large dynamic range [1]–[8]. Arrays connected electrically in series have the advantage that the voltages from the individual SQUIDs add, which yields a much larger voltage response than that obtained from a single SQUID. The larger voltage modulation in magnetic field eases requirements for unlocked direct detection, which significantly increases the bandwidth of the sensor. One disadvantage of using an array for sensing is that the overall sensor area can become quite large as more SQUIDs are added to the array. This places a practical limit on

Manuscript received December 28, 2019; revised May 11, 2020; accepted June 16, 2020. Date of publication June 23, 2020; date of current version July 3, 2020. This work was supported in part by UCOP MRPI under Grant MRP-17-454755, and in part by AFOSR under Grant FA955015-1-0218 and Grant FA9550-17-1-0096, and in part by NSF under Grant 1664446. This article was recommended by Associate Editor H. Rogalla. (*Corresponding author: Shane A. Cybart.*)

Ethan Y. Cho and Shane A. Cybart are with the Department of Electrical and Computer Engineering, University of California Riverside, Riverside, CA 92521 USA (e-mail: cybart@ucr.edu).

Jay C. LeFebvre is with the Department of Physics, University of California Riverside, Riverside, CA 92521 USA.

R. C. Dynes is with the Department of Physics, University of California, San Diego, CA 92093 USA.

Color versions of one or more of the figures in this article are available online at https://ieeexplore.ieee.org.

Digital Object Identifier 10.1109/TASC.2020.3004311

the upper frequency of operation because the sensor becomes a distributed element sensor when its dimensions are of the order of the wavelength of the signal being detected. In this article, we present a square micro-SQUID array sensor with a linear dimension of just 100 μ m per side corresponding to a lumped element quarter wave frequency of 75 GHz.

II. EXPERIMENT

To fabricate micro-SQUID arrays, we chose to utilize high transition temperature superconductor (high- $T_{\rm C}$) ion irradiated Josephson junctions fabricated with a focused helium ion beam (He-FIB) [9]. This junction technology is very flexible and conducive to high-density junction designs [10], [11]. Furthermore, helium-irradiated Josephson junctions (HI-JJ) typically exhibit larger $I_{\rm C}R$ products [12] than prior-art masked ion damage junctions [13], [14], where $I_{\rm C}$ is the critical current and R is the voltage state resistance.

We started with 25-nm-thick YBCO thin films grown by reactive coevaporation [15] on sapphire substrates by Ceraco GmbH. A 200 nm layer of gold was deposited by thermal evaporation for electrical contacts. Large features, such as electrodes and SQUID loops, were patterned with photolithography and argon ion milling. Fig. 1 shows an optical picture of the device in a square area with side $100 \, \mu \text{m}$. The array contains 84 SQUIDs connected in series, each with area $5 \times 5 \,\mu\text{m}^2$ and spacing of 5 μ m. The Josephson junctions were created by scanning a 31-keV helium ion beam from top to bottom across each loop to deliver an irradiation dose of $6 \times 10^{16} \text{ions/cm}^2$ in a field of view of 100 μ m. Arrays were created using both 20- and 5- μ m beam apertures (samples A₂₀ and A₅). Changing from a larger to smaller aperture has the effects of reducing the beam current and diameter. For this experiment, the beam currents for the 20 and 5 μ m apertures were measured using the in-column Faraday cup to be 8.4 and 0.8 pA, respectively. We estimate the beam diameters to be 2 and 0.5 nm for the 20 and 5 μ m apertures, respectively.

III. RESULTS AND DISCUSSION

Samples were cooled in an evacuated pumped nitrogen cryostat and measured from 77 to 45 K to determine the optimum operation temperature—where the dc-biased array exhibited a maximum voltage response to magnetic field. For samples A_{20} and A_{5} , the operation temperatures were found to be 65 and 52 K, respectively. Current–voltage characteristics (I-V) are shown at these temperatures for both devices in Fig. 2.

1051-8223 © 2020 IEEE. Personal use is permitted, but republication/redistribution requires IEEE permission. See https://www.ieee.org/publications/rights/index.html for more information.

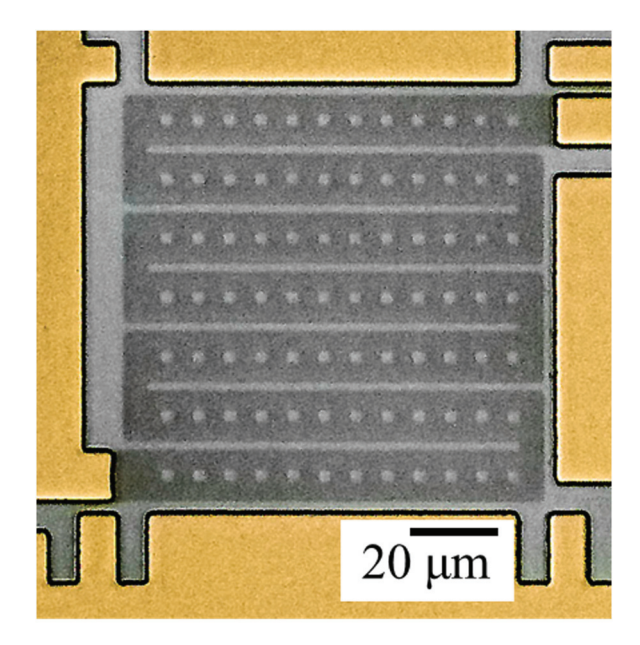


Fig. 1. Optical image of an array showing 84 SQUIDs connected in series with a meander line. Josephson junctions were directly written into the material by scanning a focused helium ion beam over each of the loops from top to bottom.

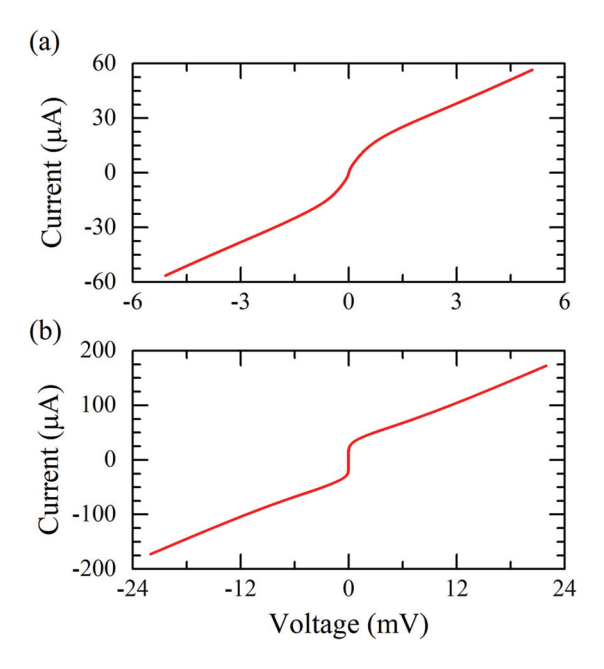


Fig. 2. (a) I-V of A_{20} that operates at 65 K with resistance of 117 Ω . (b) I-V of A_5 at 52 K with resistance of 160 Ω .

The I-V characteristics of A_{20} [see Fig. 2(a)] exhibit an average SQUID critical current of approximately 15 μA and average junction resistance of 2.8 Ω for a junction $I_{\rm C}R \sim$ 42 μV . Near zero voltage, the characteristic has pronounced rounding likely due to both nonuniformity in critical currents and thermal noise. The Josephson binding energy $(E_{\rm J})$ is of the order of the environmental thermal energy $(k_{\rm B}T)$ at this temperature [16].

In contrast, Fig. 2(b) shows I-V of sample A_5 . This array required cooling to lower temperature but exhibits much better critical current uniformity and resistively shunted junction characteristics. The average junction voltage state resistance for

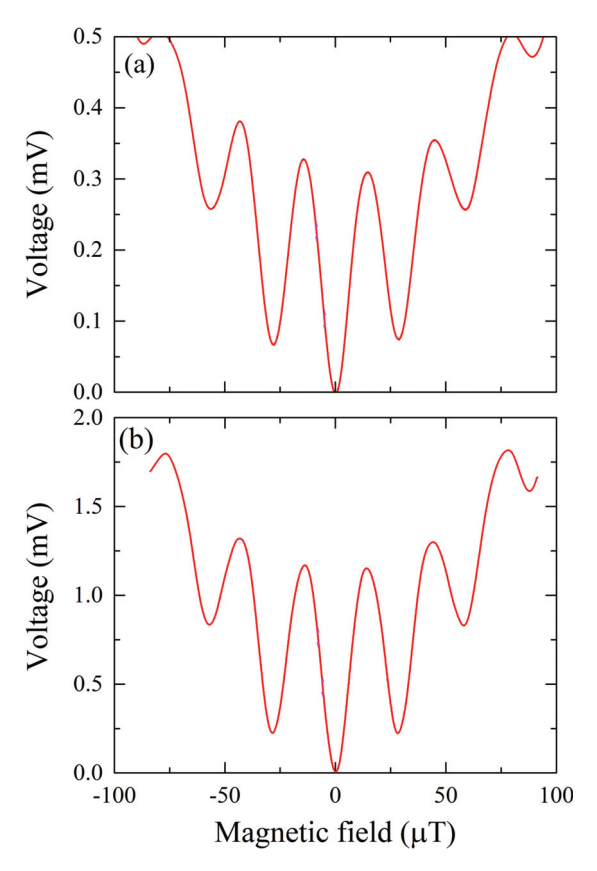


Fig. 3. (a) V-B of A_{20} array biased at 24 μA exhibiting a modulation voltage amplitude of 330 μV at 65 K. (b) V-B of A_5 current biased at 43 μA exhibiting a modulation voltage amplitude of 1.2 mV at 52 K.

 A_5 (R_{A5}) was 35% higher than that for A_{20} and found to be 3.8 Ω . This is about an order of magnitude higher than masked ion irradiated Josephson junctions [17]–[20]. We speculate that the use of the smaller aperture allows more defects to be concentrated into a smaller region that has a significant effect on electrical properties [21]. The critical currents of the junctions in this array were about 35 μ A and over a factor of 2 higher than A_{20} , yielding an average junction $I_{\rm C}R \sim$ 133 μ V. We remark that an increase in $I_{\rm C}R$ is expected when operating at lower temperatures because the superconducting energy gap becomes larger [9].

The devices were dc biased above critical current and the voltage was measured as an externally applied magnetic field was swept between $\pm 90~\mu T$. The largest amplitude of the voltage magnetic field response (V-B) was observed to be 0.33 and 1.2 mV for samples A_{20} and A_5 and is shown in Fig. 3. This factor of 3.6 difference is in good agreement with our estimates of $I_{\rm C}R$ for the two devices from Fig. 2. The magnetic field periodicity for A_{20} and A_5 were found to be 28.8 μT . This corresponds to a SQUID effective area of 70 $\mu {\rm m}^2$. We attribute the larger effective area than the physical area to be due to flux focusing from the electrodes. The maximum transfer factors for A_{20} and A_5 were found to be 35 and 132 μV μT^{-1} .

In Fig. 4, we show the critical current as a function of an external magnetic field ($I_{\rm C}$ -B) of sample A_{20} . The interference pattern from the SQUIDs as well as the junction Fraunhoffer envelope is clearly visible. The SQUID oscillation is 3.4 μ A

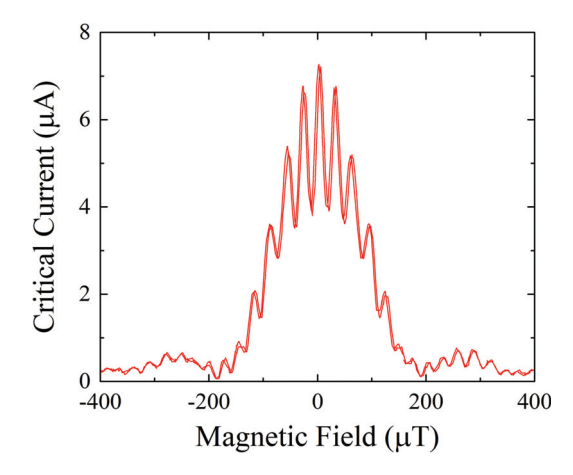


Fig. 4. Critical current modulation by external magnetic field $(I_{\rm C}-B)$ of the same array in Fig. 3(a). The plot shows two distinctive magnetic field periods for the junction and the SQUIDs at 65 K.

deep and about 45% of the total $I_{\rm C}$ modulation indicating the inductance parameter $\beta_{\rm L}=\frac{LI_{\rm C}}{\Phi_0}$ is approximately 1.2 [22] where L is 165 pH. This is much larger than what we expect for a single SQUID [23]. We attribute the larger inductance to mutual inductance between the loops [24]. From the data, we estimate the periodicity of the Fraunhoffer pattern to be $188~\mu{\rm T}$. Using the planar junction model by Rosenthal et~al. [25], $\Delta B=1.84\Phi/w^2$, this period corresponds to a junction width of 4.5 $\mu{\rm m}$, which is in excellent agreement with our lithographically defined dimension of 4.5 $\mu{\rm m}$.

IV. CONCLUSION

The data presented show that the HI-JJ process is well suited for making micro-SQUID arrays with excellent electrical properties. These devices have higher resistances than conventional broad beam masked ion irradiated junctions, which result in higher voltage output. By controlling the beam aperture and using a wider beam devices can be made for operation closer to $T_{\rm C}$. Alternatively, a smaller aperture can be utilized to create a narrower beam to make devices with higher resistance and critical current albeit at the expense of operation temperature. The direct-write helium ion YBCO single-layer process is a powerful technique for applications that require aggressive scaling to small dimensions. Such as high-frequency sensing where the size of the device should be less than the wavelength. The control afforded by the He-FIB opens up more complex geometries for high-frequency SQUID array circuits.

ACKNOWLEDGMENT

The authors would like to thank T. Wong (UCSD), A. Rondione (Oak Ridge National Laboratory Center for Nanophase Materials Sciences), and R. Stevens (Qualcomm Inc.) for technical assistance.

REFERENCES

 I. V. Vernik et al., "Cryocooled wideband digital channelizing radiofrequency receiver based on low-pass ADC," Supercond. Sci. Technol., vol. 20, no. 11, 2007, Art. no. S323.

- [2] I. V. Vernik et al., "Magnetic Josephson junctions with superconducting interlayer for cryogenic memory," *IEEE Trans. Appl. Supercond.*, vol. 23, no. 3, Jun. 2013, Art. no. 1701208.
- [3] V. K. Kornev, I. I. Soloviev, A. V. Sharafiev, N. V. Klenov, and O. A. Mukhanov, "Active electrically small antenna based on superconducting quantum array," *IEEE Trans. Appl. Supercond.*, vol. 23, no. 3, Jun. 2013, Art. no. 1800405.
- [4] S. Berggren et al., "Development of 2-D Bi-SQUID arrays with high linearity," *IEEE Trans. Appl. Supercond.*, vol. 23, no. 3, Jun. 2013, Art. no. 1400208.
- [5] J. Du et al., "Terahertz imaging using a high-T_c superconducting Josephson junction detector," Supercond. Sci. Technol., vol. 21, no. 12, Nov. 2008, Art. no. 125025.
- [6] E. E. Mitchell *et al.*, "2D SQIF arrays using 20000 YBCO high R_n Josephson junctions," *Supercond. Sci. Technol.*, vol. 29, no. 6, 2016, Art. no. 06LT01.
- [7] C. Foley et al., "Field trials using HTS squid magnetometers for ground-based and airborne geophysical applications," IEEE Trans. Appl. Supercond., vol. 9, no. 2, pp. 3786–3792, Jun. 1999.
- [8] B. Müller et al., "Josephson junctions and squids created by focused helium-ion-beam irradiation of YBa₂Cu₃O₇," Phys. Rev. Appl., vol. 11, no. 4, 2019, Art. no. 044082.
- [9] S. A. Cybart et al., "Nano Josephson superconducting tunnel junctions in YBa₂Cu₃O_{7-δ} directly patterned with a focused helium ion beam," Nature Nanotechnol., vol. 10, no. 7, pp. 598–602, 2015.
- [10] J. C. LeFebvre, E. Cho, H. Li, K. Pratt, and S. A. Cybart, "Series arrays of planar long Josephson junctions for high dynamic range magnetic flux detection," *AIP Adv.*, vol. 9, no. 10, 2019, Art. no. 105215. [Online]. Available: https://doi.org/10.1063/1.5126035
- [11] L. Kasaei et al., "Reduced critical current spread in planar MgB₂ Josephson junction array made by focused helium ion beam," *IEEE Trans. Appl. Supercond.*, vol. 29, no. 5, Aug. 2019, Art. no. 1102906.
- [12] E. Y. Cho, Y. W. Zhou, J. Y. Cho, and S. A. Cybart, "Superconducting nano Josephson junctions patterned with a focused helium ion beam," *Appl. Phys. Lett.*, vol. 113, no. 2, 2018, Art. no. 022604.
- [13] S. A. Cybart, S. M. Wu, S. M. Anton, I. Siddiqi, J. Clarke, and R. C. Dynes, "Series array of incommensurate superconducting quantum interference devices from YBa₂Cu₃O_{7-δ} damage Josephson junctions," *Appl. Phys. Lett.*, vol. 93, no. 18, 2008, Art. no. 182502. [Online]. Available: https://doi.org/10.1063/1.3013579
- [14] S. A. Cybart, S. M. Anton, S. M. Wu, J. Clarke, and R. C. Dynes, "Very large scale integration of nanopatterned YBa₂Cu₃O_{7-δ} Josephson junctions in a two-dimensional array," *Nano Lett.*, vol. 9, no. 10, pp. 3581–3585, 2009.
- [15] H. Kinder, P. Berberich, W. Prusseit, S. Rieder-Zecha, R. Semerad, and B. Utz, "YBCO film deposition on very large areas up to 20 × 20 cm²," *Phys. C*, vol. 282, pp. 107–110, 1997.
- [16] V. Ambegaokar and B. Halperin, "Voltage due to thermal noise in the DC Josephson effect," *Phys. Rev. Lett.*, vol. 22, no. 25, 1969, Art. no. 1364.
- [17] S. A. Cybart et al., "Large voltage modulation in magnetic field sensors from two-dimensional arrays of Y–Ba–Cu–O nano Josephson junctions," Appl. Phys. Lett., vol. 104, no. 6, 2014, Art. no. 062601.
- [18] S. A. Cybart, K. Chen, and R. C. Dynes, "Planar YBa₂ Cu₃ O₇ ion damage Josephson junctions and arrays," *IEEE Trans. Appl. Supercond.*, vol. 15, no. 2, pp. 241–244, Jun. 2005.
- [19] N. Bergeal, J. Lesueur, G. Faini, M. Aprili, and J. Contour, "High-T_C superconducting quantum interference devices made by ion irradiation," *Appl. Phys. Lett.*, vol. 89, no. 11, 2006, Art. no. 112515.
- [20] N. Bergeal et al., "Using ion irradiation to make high-T_C Josephson junctions," J. Appl. Phys., vol. 102, no. 8, 2007, Art. no. 083903.
- [21] E. Cho, K. Kouperine, Y. Zhuo, R. Dynes, and S. Cybart, "The effects of annealing a 2-dimensional array of ion-irradiated Josephson junctions," *Supercond. Sci. Technol.*, vol. 29, no. 9, 2016, Art. no. 094004.
- [22] C. D. Tesche and J. Clarke, "DC SQUID: Noise and optimization," J. Low Temp. Phys., vol. 29, nos. 3–4, pp. 301–331, 1977.
- [23] H. Li, E. Y. Cho, H. Cai, Y.-T. Wang, S. J. McCoy, and S. A. Cybart, "Inductance investigation of YBa₂Cu₃O_{7-δ} nano-slit SQUIDs fabricated with a focused helium ion beam," *IEEE Trans. Appl. Supercond.*, vol. 29, no. 5, Aug. 2019, Art. no. 1600404.
- [24] T. N. Dalichaouch, S. A. Cybart, and R. C. Dynes, "The effects of mutual inductances in two-dimensional arrays of Josephson junctions," *Supercond. Sci. Technol.*, vol. 27, no. 6, 2014, Art. no. 065006.
- [25] P. A. Rosenthal, M. Beasley, K. Char, M. Colclough, and G. Zaharchuk, "Flux focusing effects in planar thin-film grain-boundary Josephson junctions," *Appl. Phys. Lett.*, vol. 59, no. 26, pp. 3482–3484, 1991